The Screen Printing Analysis of Solar Panel Manufacturing

Yi Chun Tsai

Problem report submitted to the
College of Engineering and Mineral Resources
at West Virginia University
in Partial fulfillment of the requirements
for the degree of

Master of Science
in
Industrial Engineering

Majid Jaraiedi, Ph.D., Chair
Robert Creese, Ph.D.
Feng Yang, Ph.D.

Department of Industrial & Management Systems Engineering

Morgantown, West Virginia
2011

Keywords: Solar Cell, Screen Printing, ANOVA

Abstract

The Screen Printing Analysis of Solar Panel Manufacturing

Yi Chun Tsai

Statistical analysis is a powerful tool used in many walks of life, including the design of experiments to optimize process parameters and quality engineering. The goal of this research was to apply design of experiments to solar cell manufacturing process to explore the choice of methods, material and temperature on solar cell conversion efficiency. In this document a brief introduction to the principles of solar power, current solar cell manufacturing practices and various production methods is presented. Production and conversion efficiency data were collected at Ever Energy Corporation in collaboration with engineers and production staff at the company. Statistical Analysis System (SAS) package was used for data analysis and interpretation of the results. It was concluded that the optimal finger printing form is Method 1, i.e. 65 fingers, 80 μm in width and 153 mm in length, which contradicts what was suggested by the R&D engineers at Ever Energy Corporation. Also, use of the old type of paste (PV145) rather than switching to the new paste (PV159) was recommended. Superiority of PV145 compared to PV159 was shown to be statistically significant. Moreover, the results of ANOVA demonstrated that the temperature itself and the interactions between the types of paste used on the solar panel and temperatures are insignificant factors in the production line. Thus, in order to save energy, a lower temperature within the acceptable range was recommended. These results support the use of statistical methods in data analysis, and provide new insights that can be utilized advantageously by Ever Energy Corporation and similar manufacturing companies in the future.

TABLE OF CONTENTS

TABLE OF CONTENTS iii
LIST OF TABLES v
LIST OF FIGURES vi
1. Introduction 1
1.1 Introduction 1
1.2 Background of Active Solar Energy 3
1.3 Types of Solar Cells 4
1.4 The Reliability of Various Types of Solar Cells 5
1.4.1 Disadvantages of thin film solar cells 5
1.4.2 The advantages of crystalline solar cell 6
1.5 Motivation and Research Objectives 7
1.6 Methodology 9
2. Theory for Photovoltaic Transform 11
2.1 Solar Spectrum 11
2.2 The Principle of Solar Cell 14
2.3 Solar Cell Structure 19
2.3.1 Substrate 19
2.3.2 Absorber layer 20
2.3.3 Anti-reflective layer 20
2.3.4 Electrode 21
2.4 Equivalent Circuit of Solar Cell 23
2.5 Efficiency of Solar Cell 24
3. Solar Cell Manufacturing Process 27
3.1 Texturing 27
3.2 Diffusion 28
3.3 PSG Etching 28
3.4 Plasma Enhanced Chemical Vapor Deposition (PECVD) anti-reflecting coating 29

3.5 Printing and Firing 30
3.6 Edge Isolation 32
3.7 Testing/Sorting 33
4. Data Analysis of Screen Printing Process 34
4.1 Solar Cell Photovoltaic Generating Surface 34
4.2 Solar Cell Screen Printing 36
4.2.1 Number of fingers 36
4.2.2 Comparison of Numbers of Fingers 38
4.2.3 Comparison of Pastes 41
4.2.4 Comparison of Pastes at Different Temperature Values 44
4.3 Result and Discussion 47
5. Conclusions and Future Work 49
6. References 51
7. Appendix 53
Appendix 1 53
Appendix 2 54
Appendix 3 55

LIST OF TABLES

Table 1.1 Efficiency of various solar cell types 5
Table 4.1 Three kinds of fingers printing methods 37
Table 4.2 The ANOVA table for finger printing methods 39
Table 4.3 The ANOVA table for finger printing methods 40
Table 4.4 The ANOVA table for pastes selection 43
Table 4.5 The ANOVA table for pastes selection 44
Table 4.6 The ANOVA table for two pastes and three temperatures 46
Table 4.7 The ANOVA table for PV, Temperatures and their Interaction 47

LIST OF FIGURES

Figure 2.1 Black body radiation AM0 and AM1.5 11
Figure 2.2: Radiation illustration 12
Figure 2.3 Solar spectrum AM0、AM1 and AM(cscθ) 13
Figure 2.4 AM1.5G and AM1.5D spectrum 14
Figure 2.5 P-N junction under light projected 16
Figure 2.6 Open circuit voltage principle 17
Figure 2.7 Short circuit principle 18
Figure 2.8 n+pp+ energy belt of the solar cell with BSF 22
Figure 2.9 The equivalent circuit of a solar cell 23
Figure 2.10 The realistic equivalent circuit of a solar cell 23
Figure 2.11 (a) I-V curve in the solar cell and load; (b) The power generated at the maximum power point 25
Figure 3.1 The front surface of a solar cell 31
Figure 3.2 The back surface of a solar cell 31
Figure 3.3 Illustration of the distance from edge 32
Figure 3.4 Illustration of edge isolation 33
Figure 4.1 Solar cell surface with fingers and busbars 35
Figure 4.2 Solar cell back side with two busbars 36

List of Nomenclature

AM = Air mass, W/m^2.
AM 0 = Air mass spectrum in the atmosphere, W/m^2.
AM 1.5 = Air mass spectrum above the earth surface, W/m^2.
AM 1 = Air mass spectrum projected to earth surface, W/m^2.
AM 1.5D = Air mass direct incident part, W/m^2.
AM 1.5G = Air mass incident direct part and diffuse part, W/m^2.
SCL = Space charge layer
V_{oc} = Open circuit voltage, V.
L_h = Diffusing distance for electron holes, μm.
L_e = Diffusing distance for electrons, μm.
BSF = Back Surface Field
R_s = Series resistance, Ω.
R_{sh} = Shunt resistance, Ω.
I_d = Currents, A/m^2.
I_{ph} = Photon flux, eV.
I_0 = Diode saturation current in p-n junction, A/m^2.
K = Boltzmann constant, J/K.
q = Electron charge, C (coulomb).
n = Ideal factor
V_m = Maximum voltage point, V.
P_{max} = Maximum power point, W/m^2.
I_{sc} = Short circuit current, A.
P_{in} = Intensity of the projected light, W/m^2.
IPA = Isopropyl alcohol

1. Introduction

1.1 Introduction

In recent decades the consumption of traditional energy sources, such as gas, coal, and oil has increased dramatically due to heavy demand. The over-consumption of these natural sources has caused the prices to soar. As a result, the costs of production have increased drastically accordingly. At times, shortage of natural sources has turned into energy crisis. Also, the exhaust gases that are generated from traditional energy types has had a severe impact on the environment. The exhaust gases, or so-called green house gases, have increased environmental stress, leading to ecological disasters. Furthermore, the exhaust gases have been hypothesized to contribute to global climate change. To date, scientists have been conducting research to find a solution to this problem. Studies on greener, renewable energy sources, such as wind, water, solar energies have been booming in the recent years. All renewable energy types are sourced from solar energy. Solar energy, radiant light and heat from the sun, has been utilized by humans since ancient times. Solar radiation along with intermediate solar-powered resources such as wind and wave power, hydroelectricity and biomass, account for most of the available renewable energy on earth. With such great potential, only a minuscule fraction of the available solar energy is used. Solar technologies are broadly characterized as either passive solar or active

solar depending on the way they capture, convert and distribute solar energy. Active solar techniques include the use of photovoltaic panels and solar thermal collectors. Passive solar techniques include orienting a building to the sun, selecting materials with favorable thermal mass or light dispersing properties, and designing spaces that naturally circulate air. The Earth receives 174 petawatts (PW) of incoming solar radiation (insolation) at the upper atmosphere. Approximately 30% is reflected back to space while the rest is absorbed by clouds, oceans and land. Earth's land surface, oceans and atmosphere absorb solar radiation, and this raises their temperature. Warm air containing evaporated water from the oceans rises, causing atmospheric circulation or convection. When the air reaches a high altitude, where the temperature is low, water vapor condenses into clouds, which rain onto the Earth's surface, completing the water cycle. The latent heat of water condensation amplifies convection, producing atmospheric phenomena such as wind, cyclones and anti-cyclones. Sunlight absorbed by the oceans and land masses keeps the surface at an average temperature of 14 °C. By photosynthesis green plants convert solar energy into chemical energy, which produces food, wood and the biomass from which fossil fuels are derived. The total solar energy absorbed by Earth's atmosphere, oceans and land masses is approximately 3.85×10^{24} Watts per year. In 2002, this was more energy in one hour than the world used in one year. The amount of solar energy reaching the surface of the planet is so vast that in one year it is about twice as much as will ever be obtained from all of the Earth's

non-renewable resources of coal, oil, natural gas, and mined uranium combined. Solar energy can be harnessed in different levels around the world.

1.2 Background of Active Solar Energy

Solar energy can be generated anywhere in the world with sufficient sunlight. Therefore, solar energy serves as optimal candidate as a new energy source because it cannot be monopolized by a single country or an energy company. Furthermore, the total solar energy from solar radiation is as high as 1.7×10^{17} Watts [1]. The endless resources would be sufficient to cover the world's demands even if merely one millionth percent is successfully transferred [2]. Comparing to other sources of renewable energy, solar energy started out early and has been utilized in more applications. Currently there are a lot of solar panels installed in various regions of the world [3, 4].

Despite the almost infinite solar energy sources, the usage of active solar energy has been restricted by the efficiency of collecting technologies. Broad varieties of solar energy collecting methods have been developed, but the collecting efficiency remains low. Thus, the purpose of this research is to improve solar cells' photovoltaic efficiency through improving the manufacturing process, which is predicted in a statistic model. The objective is to optimize manufacturing process and further reduce manufacturing costs. Besides, another reason to expand the generation of solar energy is that these solar cells are composed of silicon. Since 20% of the earth is composed of this abundant element, the technology

used at semi-conductor factories which use silicon is highly advanced, well ahead of the technology for other renewable sources of energy. Thirdly, it is well known in the semi-conductor field that the secondary silicon wafer form these semi-conductor companies can be re-used in the solar cell manufacturing. For example, semi-conductor companies use extremely purified silicon wafers which contain 9n (99.9999999%). But what if the silicon wafer were not purified enough for semi-conductor manufacturing? The solar cell manufacturing process still can endure the secondary purification which is 6n (99.9999%). Thus, the resource used in solar cell manufacturing is directly derived from the semi-conductor field and this resource will not influence the original supply quantity due to fact that the resource is secondary wafer which cannot be used in semi-conductor field.

1.3 Types of Solar Cells

There are mainly two different types of solar cells, bulk and thin film. For bulk solar cell, it can be sorted into three different types, monocrystalline silicon wafer, polycrystalline silicon wafer and III-V type composition. Thin film solar energy, includes amorphous silicon (a-Si), CdTe, CIS (Copper Indium Diselenide)/CIGS (Copper Indium Gallium Diselenide) and nanocrtstalline silicon (ni-Si or Microcrystalline silicon mc-Si). Table 1 lists the efficiency of various types of photovoltaic sources [5].

Table 1.1 Efficiency of various solar cell types

Type	Solar Cell		Efficiency (%)
Bulk	Monocrystalline		16-24
	Polycrystalline		12-19
	III-V type	GaAs	24-25
		AlGaAs/GaAs Tandem	>25
Thin Film	Amorphous Silicon		12-19
	CdTe		15-16
	CIS(Copper Indium Diselenide)		17-19

1.4 The Reliability of Various Types of Solar Cells

1.4.1 Disadvantages of thin film solar cells

In the more recent development of solar panels, bulk solar panels are becoming more popular. The crystalline solar energy, including monocrystalline and polycrystalline silicon panels account for up to 80% of all types of solar cells. Although the other bulk solar panel, III-V type solar cell has higher photovoltaic efficiency, the use of III-V type solar energy is restricted by its relatively higher cost. In addition, a solar concentrator is required when a III-V type solar cell is used [3]. Therefore, this high performance solar technique can only be used in critical situations and facilities, such as in a satellite. For thin film solar cells, manufacturing cost is low. However, there are still technical issues that need to be resolved

before mass production becomes economical. First of all, the pollution caused in the manufacturing process is of high concern. Te is a very toxic pollutant that does not decompose in the process. Secondly, the photovoltaic efficiency transferred by thin film is still much lower than crystalline solar energy. Thirdly, photovoltaic collapse reduces photovoltaic efficiency of thin film solar cells over time. Finally, the compounds used in thin film manufacturing are much rarer than the crystalline solar cells. These compounds are difficult to synthesize, and therefore the costs to collect these compounds are high. Due to the aforementioned reasons, production of thin film solar cell remains at laboratory scale.

1.4.2 The advantages of crystalline solar cell

Crystalline solar cells have been commercialized and are broadly used. Crystalline solar cells are more popular than others are due to the following reasons. First, the background of crystalline solar cell manufacturing is more developed and its production has fewer limitations. The manufacturing techniques are the same as the semi-conductor field. From crystal growth, wafer manufacturing to p-n junction technique, the background of both semi-conductor field and solar cell manufacturing field are very similar. For example, one of the key steps in solar manufacturing is PECVD (Plasma-enhanced chemical vapor deposition). The principle of this process is the same with semi-conductor manufacturing process. Even though the applications of solar cells and semi-conductors are different, one

may find that some of the manufacturing processes of two techniques can even share the same machine. This also reduces the manufacturing costs since the development of new machines may be expensive. Therefore, the same technique has been used for more than 10 years. Secondly, crystalline solar cells generally exhibit higher PV efficiency than thin film solar cells. For example, monocrystalline solar cells exhibit as high as 24% efficiency under the laboratory circumstance [6]. The efficiency for mass production for the monocrystalline solar cells also can get as high as 15% to 18% [7]. In addition, the efficiency of polycrystalline solar cell get to 19.8% in laboratory and 13%-16% in commercial application [8, 9]. Thirdly, crystalline solar cells remain as a stable source of electric power generation. No photovoltaic collapses occur over time. With current crystalline solar cell on the market, electricity is generated for twenty years without interruption.

1.5 Motivation and Research Objectives

Recently, the price of oil has going up dramatically which has had a negative impact on all kinds of economic activities. For example, food became more expensive, people in Russia almost cannot afford heater, people decrease their traveling activities because of high gasoline price, etc. Therefore, a substitute energy plan to decrease gasoline consumption should result in a decrease in the price of gasoline. According to the above factors, the first priority in solar energy is to invest resource to decrease its manufacturing cost and also to improve its photovoltaic efficiency. In the past twenty years, scientists have improved solar

efficiency and cut down the relative costs, but the cost for every unit Watt is still at $2.5/watt~$3.0/watt [10]. This cost range is still a lot higher than the electricity generated by traditional power. The efficiency of the solar technique is about 15%. In other words, solar power only has 15% transferred to electricity, and rest of the energy is dissipated in the form of heat. Therefore, scientists are working on improving efficiency in various ways such as finding a different substrate. There are currently a few solar techniques that can achieve 20% efficiency. Solar cells that can achieve 20% efficiency still have some issues. High performance solar cells are used only in the specific way such as satellites. Other solar cells that are manufactured can only perform 15% efficiency on the average. In other words, these low performance solar cells only can transform 15% of the heat to electricity; the other 85% heat would diminish without any beneficial use. Therefore, how to improve efficiency is a hot research topic for scientists. Besides, except for improving the efficiency, the other goal is to lower manufacturing cost so that it can become economical enough for use all over the world.

The objectives of this research are to find the best combination of various materials and screen printing methods. In order to achieve the highest value of efficiency, three screen printing methods and two pastes will be considered in this study. Statistical technique such as ANOVA will be used to explore the difference among screen printing methods and pastes.

1.6 Methodology

In this research, several experimental data sets will be used in the selection of the best screen printing methods and material types. Three types of screen printing methods and two pastes tested in the manufacturing process will be considered. The methodology to be followed is:

1. Perform a thorough search of the literature in the solar energy generation field.
2. Secure the cooperation of a company in the solar energy field to allow collection of needed data. The company targeted is Ever Energy Corporation in Taiwan.
3. Obtain data from an experimental design that was run by the collaborator in the company.
4. Perform statistical analysis of the data
5. Interpret the results and make recommendations

In order to follow the above methodology, the following tasks are identified:

Task 1: Analyze the solar cell market and demand

In this section, the reason that solar cell modules are widely used around the world will be discussed. Also, the relative merit of other renewable energies will be discussed.

Task 2: Introduce the solar cell transform theory

The essential theory to transfer the projected light to electricity will be briefly discussed. The description would include citations from the literature and the formula used in the theory.

Task 3: Introduce the solar cell manufacturing process

In this step, the solar cell manufacturing process will be described, including the theory and the factors in each step. Besides, related chemical formula used in each machine will also be explained.

Task 4: Analyze experimental data by using ANOVA

This step includes a description of the experimental data sets, statistical model, results of ANOVA and the interpretation of the results of the statistical analysis.

2. Theory for Photovoltaic Transform

2.1 Solar Spectrum

To calculate the amounts of solar energy, a solar spectrum is used. In a solar spectrum, a black body radiation of temperature 6,000K is utilized. The electromagnetic wave irradiates to the earth and the spectral intensity is measured at a various wavelengths. The spectral intensity is recorded and is shown in Figure 2.1[1]. In this figure, AM0 represents the spectrum that is detected outside atmosphere and AM1.5 represents the spectrum that is detected inside atmosphere. The reason that solar spectra are different inside and outside atmosphere is due to the absorption and deflection of electromagnetic waves (irradiation) by earth's atmosphere.

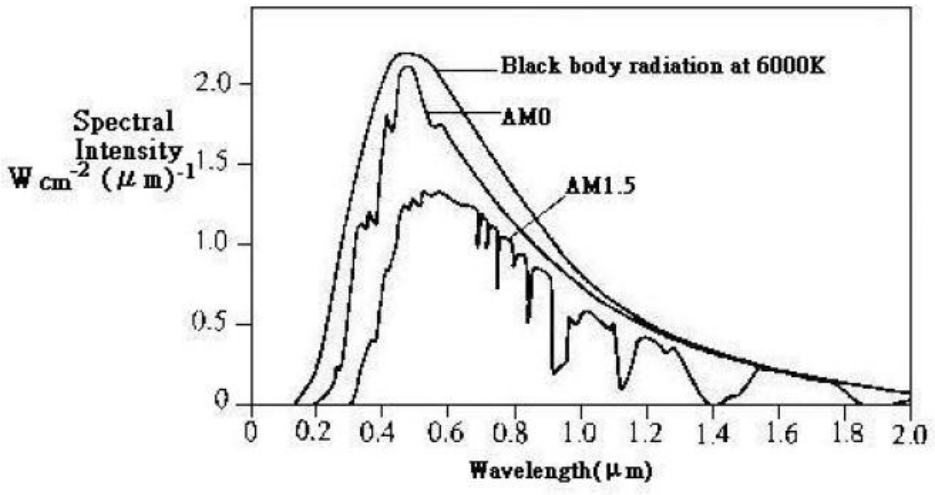

Figure 2.1 Black body radiation AM0 and AM1.5

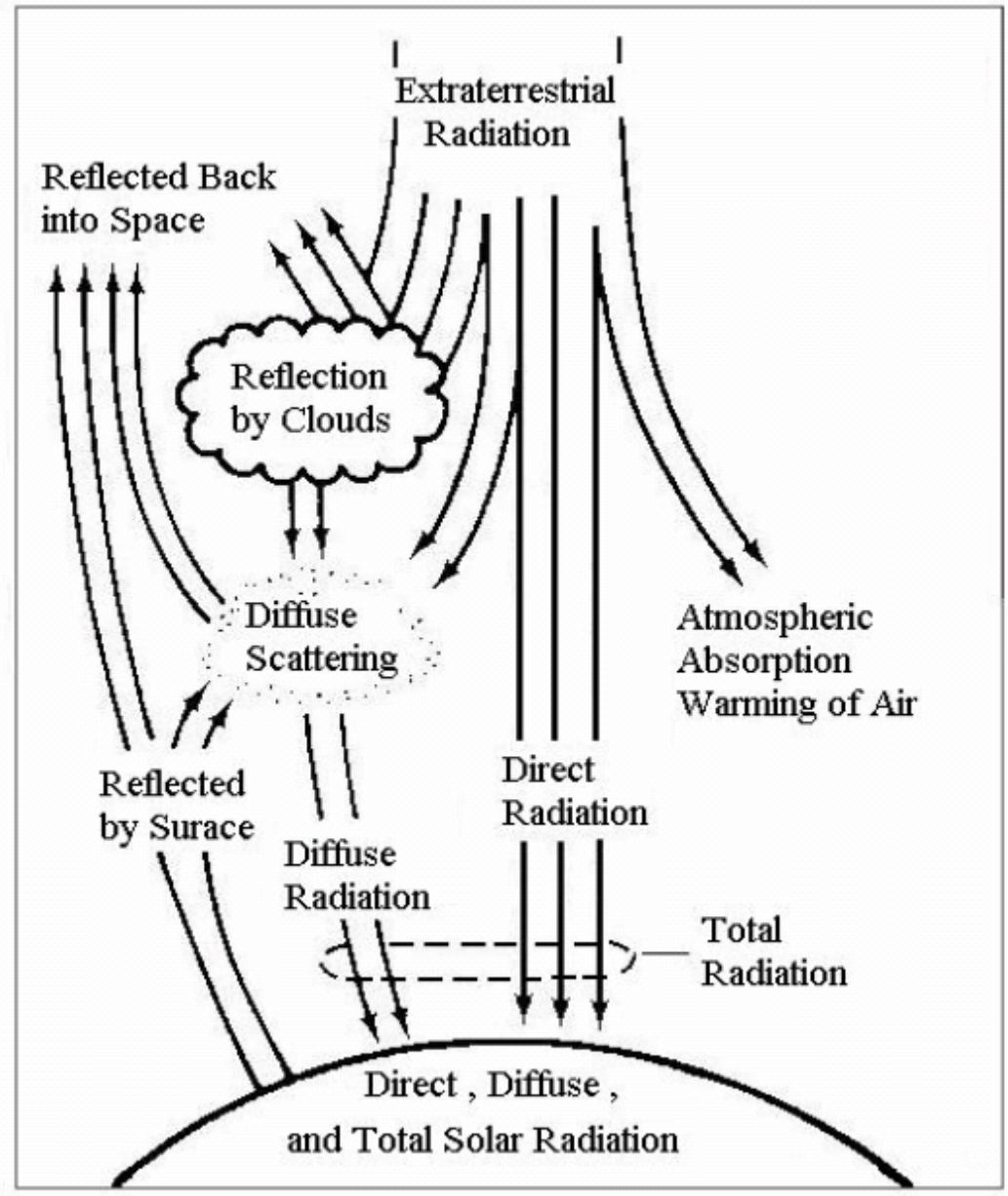

Figure 2.2: Radiation illustration

As shown in Figure 2.2 [1], solar radiations are absorbed and diffused by the earth's atmosphere while only portion of solar radiation passes through the atmosphere to the earth. For example, the water molecules in the air absorb solar energy which influences the spectral intensity at wavelengths 900, 1100, 1400 and 1900 nanometers. Carbon dioxide absorbs

solar energy at wavelengths 1800 and 2600 nanometers. In Figure 2.1, it is clear that solar energy is absorbed at different wavelengths after passing through the earth's atmosphere. To calculate solar energy, the incident angle is added into consideration. It is because measurement of solar energy is influenced by the incident angle of solar radiation. Thus, a parameter, Air Mass (m) is defined to obtain the total solar energy:

$$m=\csc\theta$$

Here, the angle θ represents the incident angle of solar radiation and CSC is the cosecant operator. The solar spectrum that was used is AM1.5, which is solar spectrum inside the atmosphere. The incident angle is defined as 42°, so the total power density can be calculated from the solar spectrum in Figure 2.1. After calculation, the total power density is as high as 963 Wm^{-2}. With incident angle 42°, the standard total solar spectrum is defined as 1,000 Wm^{-2}. The spectrum outside of atmosphere is defined as AM0. The spectrum which vertically projects into the earth's surface is defined as AM1. All spectra, incident angle and definitions are shown in Figure 2.3.

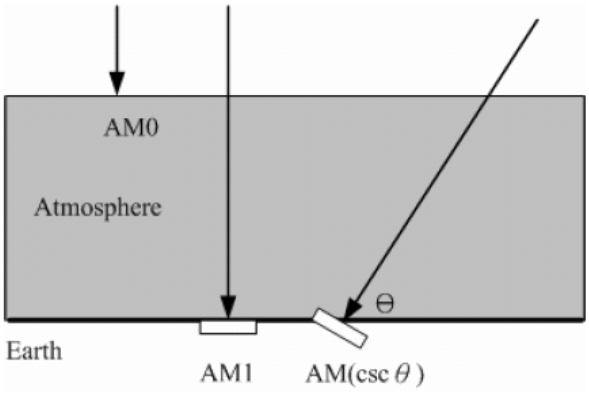

Figure 2.3 Solar spectrum AM0、AM1 and AM(cscθ)

Sometimes a letter G (represents global) or D (represents direct) is used identify a certain spectrum. For example, AM1.5D represents solar spectrum of direct incident and AM1.5G represents solar spectrum of direct incident and diffusion (shown in Figure 2.4 [1]).

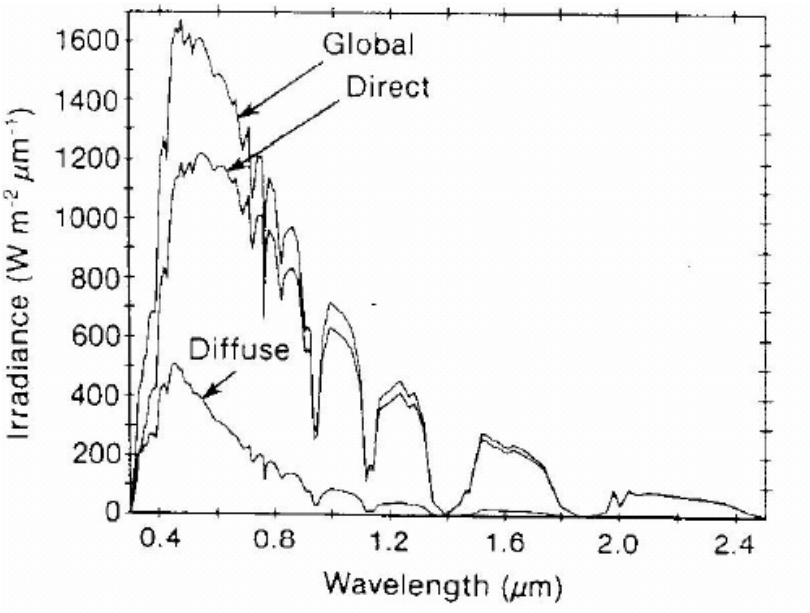

Figure 2.4 AM1.5G and AM1.5D spectrum

2.2 The Principle of Solar Cell

The fundamental semi-conductor solar cells are based on P-N junction structure [11]. The principle of p-n junction based solar cells replies on different ion density in p type and n type semiconductors. Once a semiconductor solar cell receives certain energy from radiation, electron holes from p type diffuse into n type and electrons from n type diffuse into p type due to ion density gradient. These electrons and electron holes are recombined in p type and n type semiconductors. As a result, only ionized molecules are preserved in the junction.

In p type there are negatively charged ions (acceptors). In n type there are positively charged ions (donors). The depletion of charges and space charged layer (SLC) generates a potential difference and a built-in field is formed. However, not all the energy from radiation can stimulate p type and n type semiconductors to generate holes and electrons. Different semiconductors exhibit different energy gaps that are determined by the composed materials. Only when the radiation energy (photon energy) surpasses the semiconductor's energy gap, the electrons and holes can be generated. The radiation energy that is insufficient to stimulate the formation of electrons and holes, i.e. photon energy is lower than energy gap, can only transform to thermal energy and dissipate without absorption. The energy gap in a p-n junction semiconductor and photon energy are shown in Figure 2.5 [1]. It is noted that radiation energy (photon energy) is a function of wavelength. For a semiconductor solar cell with large energy gap, only the radiation energy of smaller wavelength is absorbed. It is because the radiation of smaller wavelength exhibits higher energy. For a high efficiency semiconductor solar cell, a small energy gap is required because a larger portion of solar spectrum is utilized.

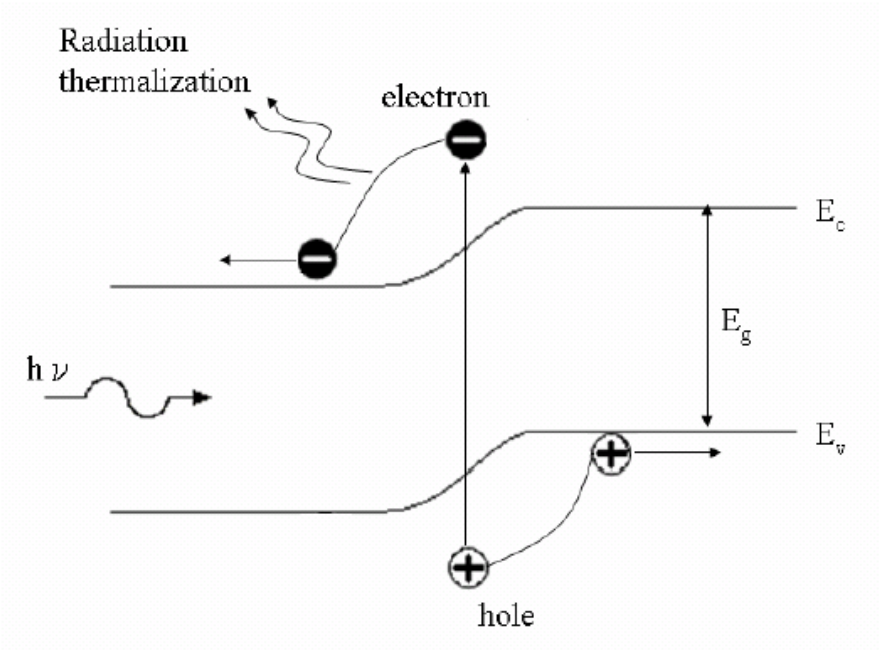

Figure 2.5 P-N junction under light projected

However, while electrons and holes are generated in the depletion region, the directions that electrons or electron holes diffuse to are driven by the potential difference between p type and n type semiconductors. Because the potentials of two semiconductors are different, the electrons have tendency diffusing to one direction and electron holes diffuse to the other direction. The accumulation of electrons and electron holes causes potential difference. At this time, the potential difference between p type and n type is defined as open circuit voltage (Voc), which is shown in Figure 2.6 [1]. The open circuit voltage is also the maximum voltage that a solar cell can achieve.

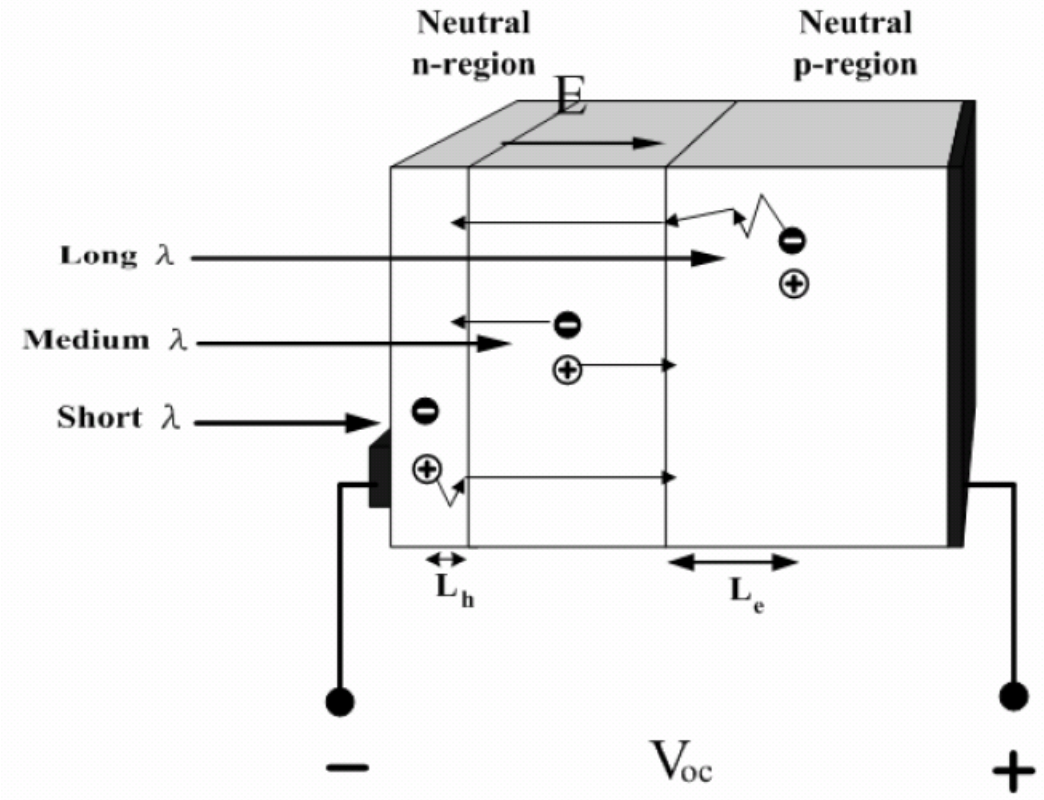

Figure 2.6 Open circuit voltage principle

In Figure 2.6, L_h and L_e are diffusing distance for electron holes and electrons respectively. It can be noticed that radiation of longer wavelength penetrate deeper and then be absorbed. It is because the absorption coefficients of a material are a function of the wavelength. The absorption coefficient of a shorter wavelength is greater than the coefficient of longer wavelength. However, the absorption depth is an inverse ratio to the absorption coefficient. As a result, a photon with shorter wavelength will be absorbed in the solar cell surface, and a photon with longer wavelength can reach deeper and then be absorbed. When short circuit occurs in the neutral N type region, the excess electrons can diffuse to the P type region to neutralize the excess electron holes by the outer short circuit (shown in Figure 2.7 [1]).

When this happens, the circuit is defined as short circuit current, I_{SC}, which is also called photocurrent, I_{ph}.

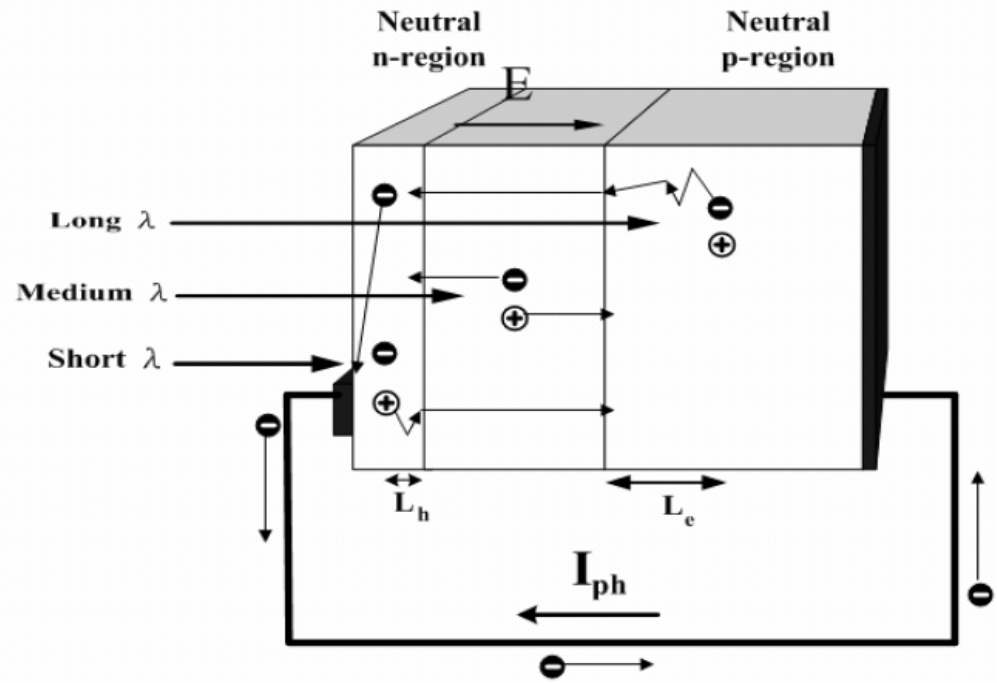

Figure 2.7 Short circuit principle

2.3 Solar Cell Structure

With the development of solar cell technology, novel materials and advanced manufacturing procedures were invented. Many solar cells of different structures have been developed. However, the fundamental structures of a solar cell could be divided into substrate, absorber layer, anti-absorber layer and electrode.

2.3.1 Substrate

Substrate is the main structure of a solar cell, which provides a support to ensure solar cell's integrity. For some types of solar cells, photovoltaic reactions take place in the substrate. In the manufacturing process, substrate is always the first structure to be made. Afterwards, other structures and layers are constructed on top of the substrate layer. The monocrystalline solar cells utilize silicon wafer as substrate. The wafer works as substrate that provides structural integrity and also serves as the absorber layer. III-V group solar cells utilize silicon wafer as substrate, too. In the manufacturing process, p type and n type semiconductors are synthesized on silicon wafer using two different epitaxy techniques. However, the substrate usually is not involved in the photovoltaic reaction. The advantage of using epitaxy techniques is that multiple structures can be established in one component. For example, heterojunction, tandem, quantum well, quantum dot, can be constructed on the same substrate. As for thin film solar cells, different materials, such as glasses, plastics, ceramics, stainless steel and metal chips can be utilized to form the substrate. The

substrates of thin film solar cells are not involved in photovoltaic reaction.

2.3.2 Absorber layer

Absorber layer is the core of a solar cell. The function of an absorber layer is to separate electrons and electron holes from semiconductor and deliver to the circuit. To do so, an electric field is formed in the absorber layer that is stimulated by the radiation energy and p-n junction. For the example of monocrystalline solar cells, the absorber layer is made of p type or n type wafer. Using high temperature diffusion technique, an n type material is diffused in a p type wafer or a p type material is diffused in an n type wafer. The purpose of using high temperature diffusion technique is to form a extremely thin layer, so the photons can penetrate through the diffusion layer to the depletion layer. It is noted that most of monocrystaline solar cells adopt n type semiconductors as absorber layer due to the fact that n type semiconductor is usually thinner than the p type. The reason that n type semiconductor layer is thinner is because the diffusion distance of carriers is shorter in n type semiconductors. The same principle explains why the p type semiconductor is usually used as substrates in monocrystalline solar cells.

2.3.3 Anti-reflective layer

The anti-reflective layer is utilized to reduce the reflection of incident solar radiation [12]. Without an anti-reflective layer, 30% of solar radiation can dissipate through reflection.

This amount of solar radiation is very crucial for a solar cell. For an anti-reflective layer, the refraction index of materials and thickness are considered. Sometimes, multiple layers are used to replace single layer depending on the function. The materials that are used in anti-reflective coating include MgF_2/ZnS, TiO_x/Al_2O_3, Si_xN_x, SiO_x and so on. Anti-reflective layer not only reduces the reflection but also protects solar cells from corrosion. It also prevents excess humidity and scratches on the panel.

2.3.4 Electrode

The electrodes of solar cells are meant to conduct currents to the exterior electric circuit. An electrode that is printed on the light exposure face is called top electrode and the electrode that is printed on the opposite face is called back electrode. Because the top electrode is exposed to the sun light, the least numbers of fingers are preferred. However, the conductivity of electrodes drops when fewer fingers are printed. As a result, the electrodes are usually printed as finger-like on a solar cell. The design is to maximize the contact area to the absorber layer and at the same time minimize the electrode's surface area. As for back electrode, it is not exposed to the sun light so the criteria for its printing format are more flexible. The selection of electrode materials is also crucial. Work function and Fermi Level of a material are considered when choosing electrode materials. A proper material forms Ohmic contact when connect with absorber layers. An adverse material forms Schottky barrier with absorber layer and voltage depletion would occur. The

electrodes are usually doped with other elements in order to adjust the electrode material's Fermi Level. In most solar cells, the materials that are used in back electrode printing exhibit higher impurity doping density than the substrate. The impurity doping causes a deviate Fermi Level with substrate. It further generates an electric field (Back Surface Field, BSF) between electrode and substrate. The Back Surface Field forms a p-n junction-like barrier to impede carrier flow to the rear surface. It reduces electron pairs recombination at solar cell's back surface and thereby increases the cell's efficiency. The principle of Fermi Level and Back Surface Field are shown in Figure 2.8 [1].

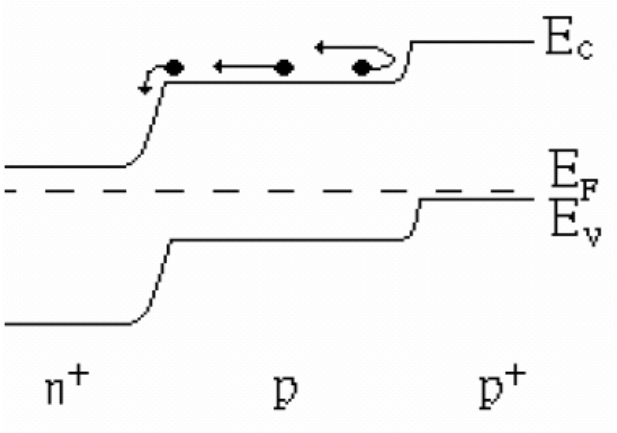

Figure 2.8 n+pp+ energy belt of the solar cell with BSF

2.4 Equivalent Circuit of Solar Cell

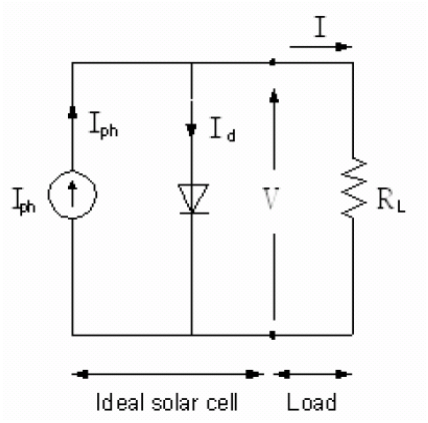

Figure 2.9 The equivalent circuit of a solar cell

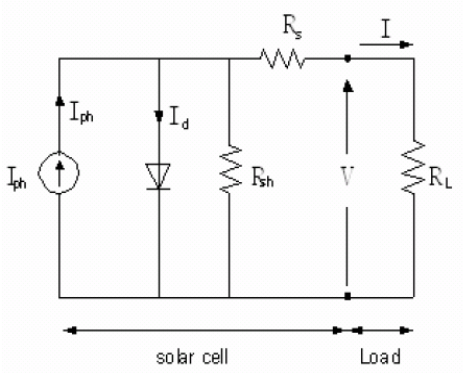

Figure 2.10 The realistic equivalent circuit of a solar cell

The equivalent circuit of a solar cell is shown in Figure 2.9 [1]. A solar cell can be seen as a current generator which generates current I_{ph}. However, a solar cell is not a perfect conductor and the resistance is always listed in the consideration when a solar cell is designed. A realistic solar cell is shown in Figure 2.10 [1], in which two distinct impedance in the solar cell, series resistance (R_s) and shunt resistance (R_{sh}) are illustrated. The series resistance is contributed by the solar cell's materials because a solar cell is mainly made of semiconductors. The shunt resistance is caused by leakage of current from one terminal to the other due to the poor insulation, defects between electrodes and semiconductor junction,

and so on. In another words, photovoltaic currents go back through the device itself or the grain boundary instead of go back to the load. For a good solar cell, a lower series resistance R_s is preferred. Instead, a higher shunt resistance R_{sh} is preferred in a solar cell, because the higher shunt resistance would allow higher photovoltaic current move to the load.

2.5 Efficiency of Solar Cell

This section introduces the calculation of a solar cell's efficiency. When a load is connected to the solar cell, the current decreases and a voltage develops as charge builds up at the terminals. The resulting current can be viewed as a superposition of the short circuit current, caused by the absorption of photons, and a dark current I_d, which is caused by the potential built up over the load and flows in the opposite direction. As a solar cell contains p-n junctions, it may be treated as a diode. Thus, the current of a solar cell can be shown as follows [10, 13]:

—

I_d = Dark currents

I_{ph} = Photon flux, eV.

I_0 = Diode saturation current in p-n junction, A/m^2.

K= Boltzmann constant, J/K.

q = Electron charge, C (coulomb).

n = ideal factor

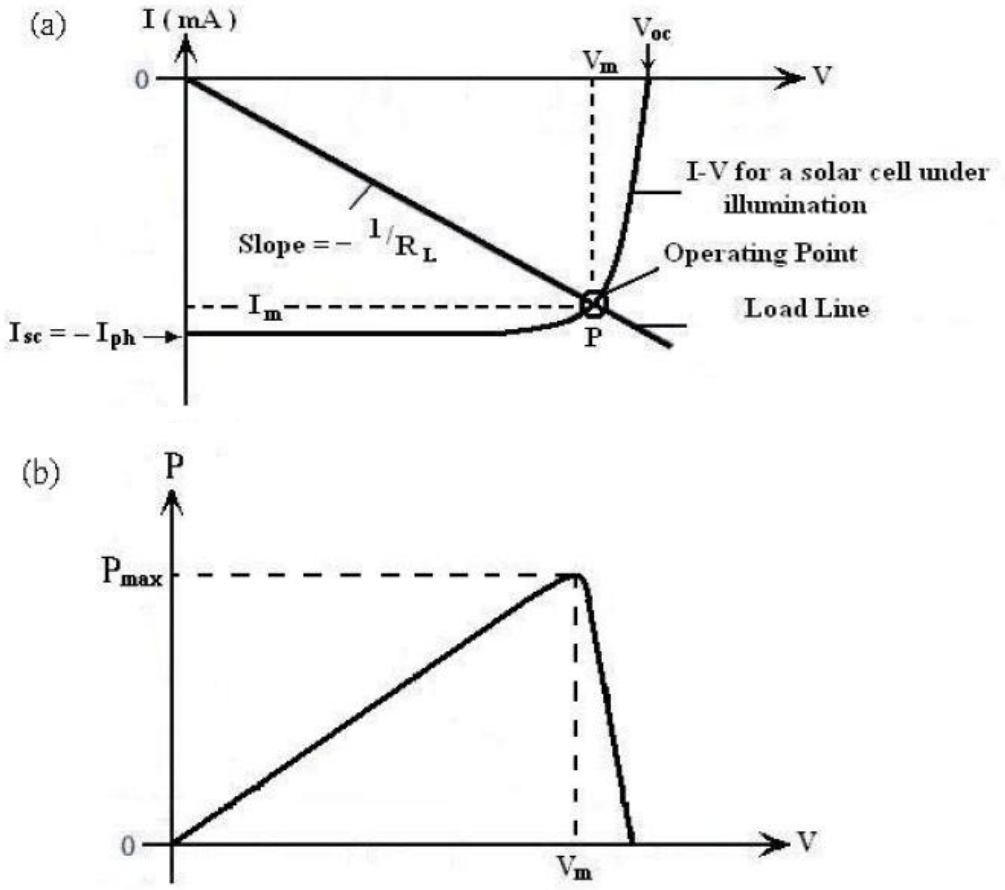

Figure 2.11 (a) I-V curve in the solar cell and load; (b) The power generated at the maximum power point

Figure 2.11 [1] shows (a) current-voltage relation and (b) power-voltage relation when the solar cell is under illumination. The maximum voltage and maximum current is determined by drawing a load line to intersect the current-voltage curve in Figure 2.11 (a). The maximum power can then be plugged into Figure 2.11 (b) to find out the maximum output power of the solar cell. The output power can expressed as below:

—

Figure 2.11(b) is the related output power and voltage characteristic curve. It has to be

differentiated for the output and voltage to get the maximum output power. Thus, it is possible to get the V_m under the maximum output circumstance:

Therefore, the maximum output power, P_{max} is:

P_{max} is the biggest area circled by the I-V curve, and it was determined as fill factor (FF):

The conversion efficiency of the solar cell is to simulate the percentage of solar spectrum being converted to electric power by the solar cell. The solar spectrum inside atmosphere, AM1.5 $^{mW}/_{cm^2}$ and 25ºC is used. The conversion efficiency η is shown in below:

$$\eta = \frac{P_{max}}{P_{in}} \times 100\% = \frac{V_m I_m}{P_{in}} \times 100\% = \frac{V_{oc} I_{sc} FF}{100\left(^{mW}/_{cm^2}\right)} \times 100\%$$

P_{in} is the intensity of the projected light equal to 100 $^{mW}/_{cm^2}$.

3. Solar Cell Manufacturing Process

In a solar cell manufacturing process, there are seven main processes in the manufacturing line. The seven stages are texturing, diffusion, PSG etching, PEVCD(Plasma enhanced Chemical Vapor Deposition) [14], printing, fast firing [15], edge isolation and testing/sorting [16]. Each process plays an important role in the manufacturing line. Each process includes hundreds of parameters. Therefore, how to adjust the parameters prior to manufacturing so a solar cell can achieve the optimal conversion efficiency is very crucial.

3.1 Texturing

In a texturing process, the first step is to clean the solar wafer. Two chemical solutions are used for cleaning including NaOH and KOH. The result of cleaning is determined by the density, temperature of solutions and cleaning time. After the wafer is cleaned, a designated texture is etched on the wafer's surface. The texture can be complicated as a reverse-pyramid shape. The purpose of texturing is to increase the surface area so the solar cell has greater exposure to solar energy. Texturing is conducted using anisotrpic etching [13]. NaOH and isopropyl alcohol (IPA) solutions are used in anisotropic etching. Anisotropic etching will cause the crystalline uncovered from the surface. In general, the degree of cleaning has a big influence on the texture quality. The density of NaOH and IPA

solutions, the temperature of solutions and etching time, all contribute to the quality of texturing.

3.2 Diffusion

This step is to form the p-n junction in the silicon wafer [17]. Normally the solar cell is composed of the p-type silicon wafer, therefore, an n-type phosphorous diffusion is performed onto the p-type silicon wafer. The most advanced method is to mix $POCl_3$ with oxygen and nitrogen in the high temperature diffusion furnace. The chemical reaction in the high temperature process is listed in below:

$$4POCl_3 + 3O_2 \rightarrow 2P_2O_5 + 6Cl_2$$

$$2P_2O_5 + 5Si \rightarrow 4P + 5SiO_2$$

In the diffusion process, phosphorus ions migrate through the silicon lattice when the system is under high temperature. At the same time a SiO_2 layer is formed on the surface. This diffusion process is also called n-type diffusion because phosphorus ions are doped into silicon wafer. In the process, the density of phosphorus ions can be determined by the nitrogen flow. Also, oxygen and nitrogen flows, time and temperature are countable to the diffusion quality. The diffusion quality is also determined by the depth of the diffusion junction, diffusion sheet resistance and dopant profile.

3.3 PSG Etching

The silicon surface reacts to the oxygen and steam, especially the thermal oxidation.

This will form a layer of silicon dioxide in the surface [10]. Normally, after the process, it would use the hydrofluoric acid (HF) to etch the exterior SiO_2. The chemical reaction is shown below:

$$SiO_2 + 6\ HF \rightarrow H_2SiF_6 + 2H_2O$$

In this process, SiO_2 is removed by HF and the final product H_2SiF_6 is dissolved in water. After the diffusion process, the p type silicon wafer is covered by an n type doping layer. Then, n-type edge is removed by using edge etching. After edge etching, the substrate is now a complete p-n junction. Usually, edge etching is conducted using plasma etching. CF_4 and O_2 are used to form the plasma etching. In this step, the quality of etching can be determined by the chip stack method, the frequency of RF and the power of RF, reacting time, gas flow of CF_4 and O_2, mixing ratio of CF_4 and O_2. If the quality of edge isolation is not desired, the shunt resistance would increase and the conversion efficiency drops.

3.4 Plasma Enhanced Chemical Vapor Deposition (PECVD) anti-reflecting coating

In the solar cell manufacturing process, Plasma Enhanced Chemical Vapor Deposition (PECVD) is used to coat an anti-reflective coating (ARC) that is composed of silicon nitride layer (SiN) [18]. The gas used in the PECVD is silane (SiH_4) and ammonia (NH_3). The chemical reaction is listed in below:

$$SiH_4 + NH_3 \rightarrow SiN{:}H + 3H_2$$

Also, SiH_4 and N_2 gas can be used. The chemical reaction is listed below:

$$2SiH_4 + N_2 \rightarrow 2SiN{:}H + 3H_2$$

SiN:H represents non-crystalline structure with hydrogen molecules adsorbed on silicon nitride's surface. In PECVD process, the frequency of RF and the power of RF, the distance between electrode and product, reacting time, temperature and pressure in the chamber and the ratio of gas flow are the crucial factors that affect the quality of anti-reflective coating. The anti-reflective coating would affect the ratio of silicon and nitride, reflection ratio, density, resistance of solar cell and energy gap of p-n junction.

3.5 Printing and Firing

After PECVD process, the p-n junction of solar cell is completed. Following the process, conductive components that connect to the device, circuits are printed. Different from the IC manufacturing process, printing solar cell circuits do not use the evaporation, physical vapor deposition or chemical vapor deposition methods. Instead, screen printing [19] and firing [20, 21] are used. It is because printing and firing are suitable for mass production. In addition, the costs of printing and firing are much lower and economic than other methods [22, 23]. To print conductive components, a metallic paste is paved on the substrate using a screen printer. For the front surface of substrate, fingers and busbars are printed as shown in Figure 3.1. As for the back surface of substrate, two busbars are printed to connect the busbars in the front surface (as shown in Figure 3.2).

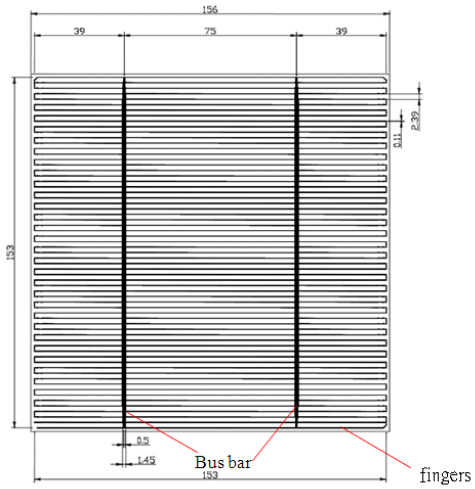

Figure 3.1 The front surface of a solar cell

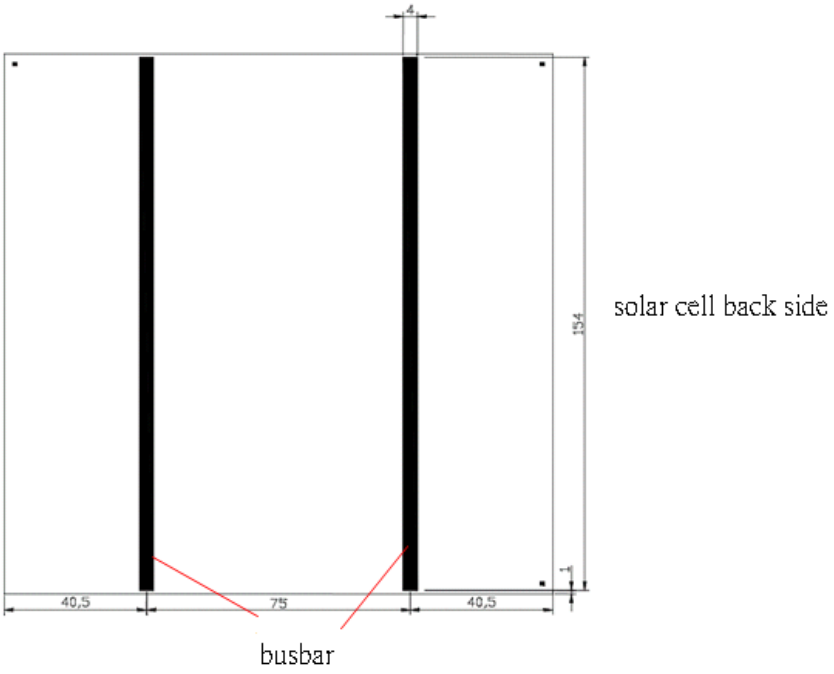

Figure 3.2 The back surface of a solar cell

After printing, the substrate is delivered to a fast firing station. In this fast firing station, the substrate was fired at the temperature higher than 860^{o}C [19]. The paste and the temperature are both very crucial factors in circuit formation. In this process, the printing format, thickness of pavement, firing temperature and time are influential in order to form a

flawless circuit.

3.6 Edge Isolation

After printing and firing, edge isolation is performed to prevent a short circuit [16, 24]. In this process, a laser is used to cut the substrate's edge in order to isolate the conduction between the front and back side. The laser makes a gap of 240μm (shown in Figure 3.3) from the edge instead of cutting off the edge. The depth of gap is around 10μm to 20μm depending on the laser's power. Figure 3.4 illustrates the depth of laser cutting in edge isolation.

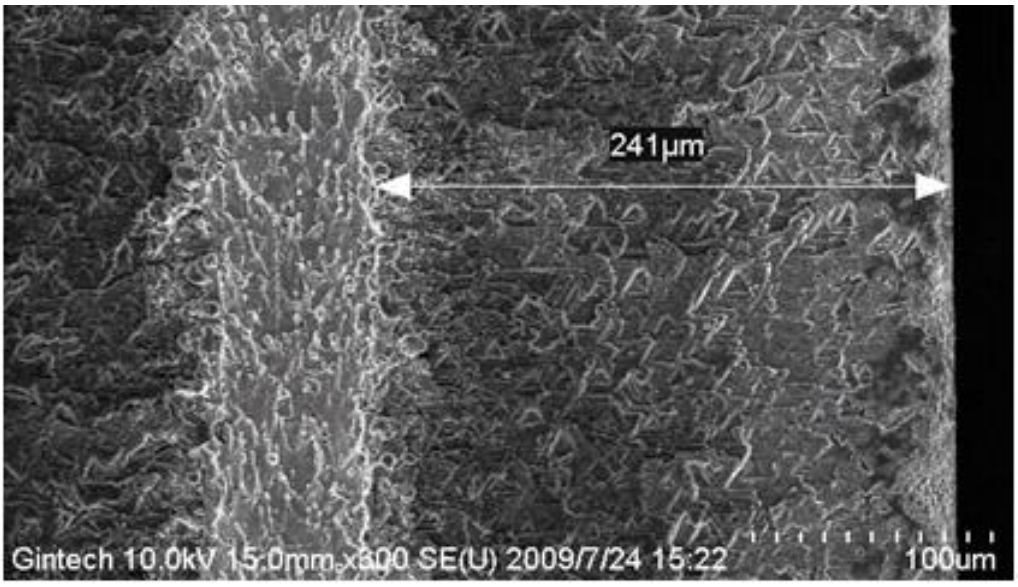

Figure 3.3 Illustration of the distance from edge

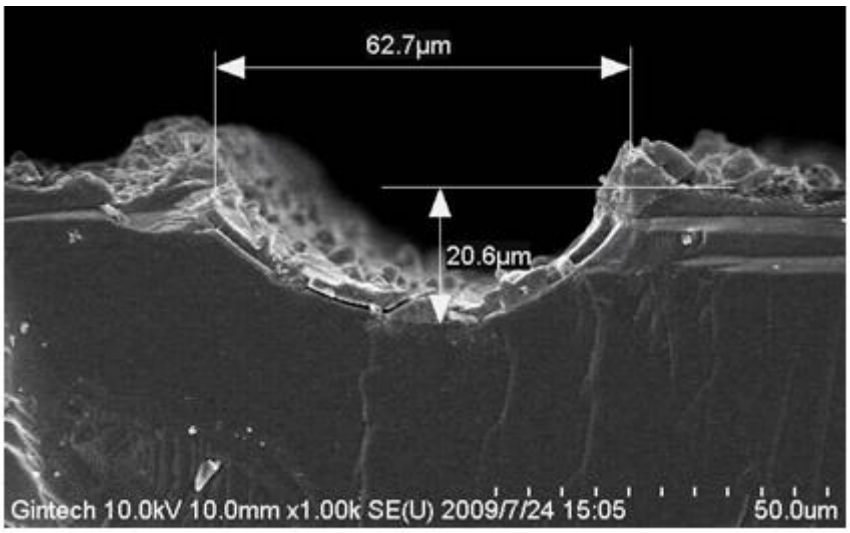

Figure 3.4 Illustration of edge isolation

3.7 Testing/Sorting

After laser isolation cutting, the next step is to test the product's conversion efficiency. In this station, the solar cell is exposed to artificial sunlight, which is simulated by an illumination machine. The conversion efficiency of solar cell is measured at this time. The conversion efficiency formula is shown as

$$\eta = \frac{P_{max}}{P_{in}} \times 100\% = \frac{V_m I_m}{P_{in}} \times 100\% = \frac{V_{oc} I_{sc} FF}{100\left(mW/cm^2\right)} \times 100\%$$

After testing, the solar cells would be sent to the sorting station. In this station, a sorting machine separates the solar cells in different trays according to the solar cells' conversion efficiency.

4. Data Analysis of Screen Printing Process

As explained before, the solar cell manufacturing procedure requires several steps. However, each station also requires a lot of time to adjust the parameters so that the solar cell can optimize the output. Therefore, there are a lot of experts who try to perform experiments in the lab to figure out the best combination of all factors involved. The solar cell output is just like the construction module that is built like a pyramid structure. As a result of research and experimentation, converting efficiency is improving every day. From the economic point of view, solar cell manufacturing process cannot be upgraded at once or optimized by using advanced calculations to get the best combination of the parameters before the start of the production of solar cells. Moreover, the manufacturing line cannot run the experiments all day without considering the costs. Therefore, although there are several very important stations that have to be upgraded, the most effective way to improve solar cell conversion efficiency is to test the paste. The paste can influence the conductivity and lower resistance so that more current can pass and enhance the overall efficiency.

4.1 Solar Cell Photovoltaic Generating Surface

Solar cell surface area is the key factor to decide the output current. Because of the projected light effect, the greater the front surface of a solar cell is the better its performance.

The larger surface contact, the more current can be produced by the p-n junction. However, in the screen printing step, the conductive electrode must be printed onto the solar cell. These conductive portions are called fingers and busbar showed in Figure 4.1. Fingers are the thinner metal paste paved like ribbons, it also can be called ribbons. Busbar means the thicker portion onto the solar cell. The solar cell surface is shown in Figure 4.1.

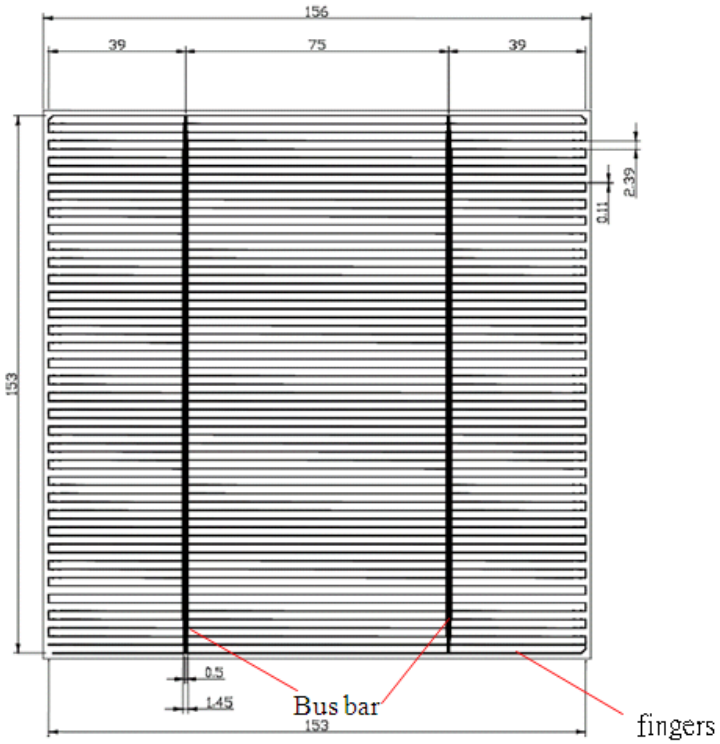

Figure 4.1 Solar cell surface with fingers and busbars

Sometimes, some special solar cells are made by three busbars. This is a special case that will not be addressed in this research. For the back side, the solar cell also needs to sinter two busbars in the back side to collect the electron holes. However, because the light does not project onto the back side, the surface area for the back side is not an important part. The only thing that has to be considered is the cost of the paste. In other words, the busbars

in the back side are the thinner the better so that it can save on the paste cost. The solar cell back side is shown in Figure 4.2, below.

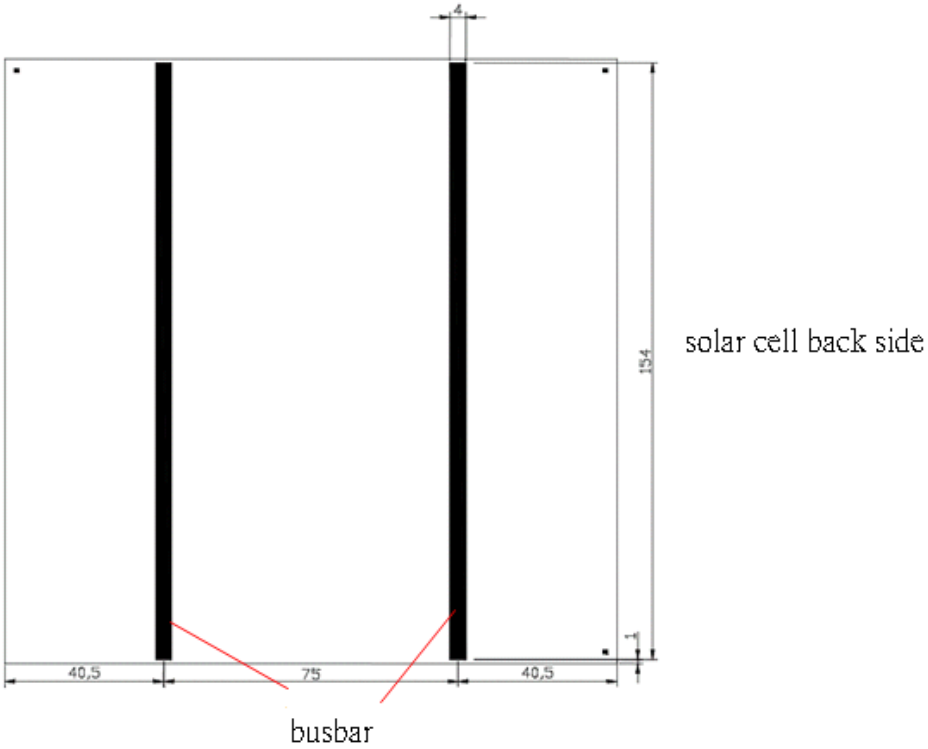

Figure 4.2 Solar cell back side with two busbars

4.2 Solar Cell Screen Printing

The solar cell surface is the key factor that affects the output. Therefore, in this step, the factors that affect the contact area will be described and explained. The goal of the experiments described below is to determine which paste can be paved in less quantity but also enhance conductivity of the solar cell.

4.2.1 Number of fingers

In modern solar cell manufacturing, a kind of paste composed of Aluminum and Silver

named PV-145 is used in the screen printing to form the conductive electrode. By using PV-145, the best result achieved, according to the R&D engineers in Ever Energy corporation, is to print 70 fingers and two busbars onto the solar cell front surface and two busbars in the back surface. In the front surface, there are 70 fingers with 70μm width and 153 mm length, two busbars with 1.45 mm width and 153 mm length. Because the surface area is the key point to influence the output current, the engineers try to figure out that if better printing formats that can reduce the fingers and also increase the output efficiency. There are three kinds of finger printing methods that need to be included in an experiment to maximize output efficiency. The three kinds of printing forms are listed in Table 4.1, below:

Table 4.1 Three kinds of fingers printing methods

Method	Numbers of Fingers	Width	Length
1	65 Fingers	80 um	153 mm
2	70 Fingers	70 um	153 mm
3	65 Fingers	70 um	153 mm

The first method is 65 fingers with 80μm width and 153 mm length. The second method is 70 fingers with 70μm width and 153 mm length. The third method is 65 fingers with 70μm and 153 mm length.

4.2.2 Comparison of Numbers of Fingers

- **Data description**

From the experimental data sets, 279 sets with different finger printing methods were selected by an Excel function. Each type of finger printing method corresponds to conversion efficiency.

- **Finger printing model**

is a constant common to all observations

are the effect of finger printing methods, = 1, 2, 3

represent the random error

represent the solar cell converting efficiency for method

Converting efficiency ( ) represents the tested converting efficiency. are random error terms that are assumed to be independently and identically distributed ~ N (0,).

- **ANOVA Table**

Data obtained from the three screen printing methods was analyzed using the SAS General Linear Model procedure. The resulting ANOVA table is shown in Table 4.2. The F value is computed as 45.95 and p-value obtained is less than 0.001which means that these three printing screen methods are significantly different from each other. This result also reveals

that the experiments for these three screen printing methods are helpful and necessary.

Table 4.2 The ANOVA table for finger printing methods

Source	DF	Sum of Squares	Mean Square	F value	Pr > F
Model	2	0.00117304	0.00058652	45.95	<.0001
Error	276	0.00352297	0.00001276		
Corrected Total	278	0.00469601			

To determine which method is the best, the following statements were used in the SAS program.

ESTIMATE 'H0: M1 = M2' METHOD 1 -1 0;

ESTIMATE 'H0: M2 = M3' METHOD 0 1 -1;

ESTIMATE 'H0: M1 = M3' METHOD 1 0 -1;

In the above statements, M1 represents the first screen printing method, M2 represents the second screen printing method, and M3 represents the third screen printing method. ESTIMATE commands are used to test the following three hypotheses: Method 1 = Method 2, Method 2 = Method 3, and Method 1 = Method 3. Table 4.3 shows the results obtained from the SAS output.

From the second column of Table 4.3 it can be seen that the estimated value of the mean difference between methods 1 and 2 is 0.00508486, the t- value is 9.59 and the p-value is less than 0.0001. Hence, it can be concluded that method 1, i.e. 65 fingers with 80 μm and 153

mm length, is significantly better than method 2.

From Table 4.3 it can also be seen that the estimate of the mean difference between methods 2 and 3 is -0.00263352, the t- value is -4.98 and the p-value is less than 0.0001. This implies that there is a significant difference between the mean conversion for method 2, i.e. 70 fingers with 70 μm and 153 mm length, and mean conversion for method 3. The same is true for testing the hypothesis; H0: M1 = M3. The difference in mean conversion for these methods is 0.00245134, the t- value is 4.77 and the p-value is less than 0.0001. According to the results, it can be concluded that method 1, 65 fingers with 80 μm and 153 mm length is significantly better than method 3.

Table 4.3 The ANOVA table for finger printing methods

Parameter	Estimate	Standard Error	t Value	Pr> | t |
H0: M1 = M2	0.00508486	0.00053046	9.59	<.0001
H0: M2 = M3	-0.00263352	0.00052916	-4.98	<.0001
H0: M1 = M3	0.00245134	0.00051435	4.77	<.0001

The confidence interval for the difference of the mean efficiency of method 1 is shown below:

The confidence interval for the difference of the mean efficiency of method 2 is shown as below:

The confidence interval for the difference of the mean efficiency of method 3 is shown as below:

4.2.3 Comparison of Pastes

The solar cell production line has more than seven machines, each of which costs several hundred thousand dollars. For achieving a higher level of efficiency, it would not be cost effective to change to a new process or a new machine without very careful consideration and analysis. Sometimes the engineers spend a lot of time trying to find a better material or a better combination of parameters which would not require any substantial change to the machines to improve the solar cell efficiency. If the R&D engineers can find a way to change the parameters or change the materials only, for example, the screen printing paste, it

will be very cost effective if the cost of the new material has a significant difference with the original one.

Recently, a new screen printing paste composed of silver and aluminum with different ratio, PV 159, was created and recommended by the supplier. The engineers cannot make this change based only on the supplier's recommendation. But the engineers are also very interested in this new paste and its potential effect on improving efficiency. Can this new paste, PV 159, outperform, PV 145, the original paste? This is the question that we address below.

Data description

Results in Section 4.2.2, indicated that the best method to print the fingers is the first method, i.e. 65 fingers with 80μm width and 153 mm length by using PV 145. Therefore, according to this result, the engineers conducted a set of new experiments using this method of screen printing method to learn about the effectiveness of the new paste. There are 255 data sets randomly selected by an Excel function. For the two different kinds of pastes, each observation represents conversion efficiency.

- **Pastes selection model**

is a constant common to all observations

are the effect of different pastes, = 1, 2

represent the random error

represent the solar cell converting efficiency for method

Conversion efficiency ( ) represents the tested converting efficiency. are the random error terms that are assumed to be independently and identically distributed ~N (0,).

- **ANOVA Table**

From Table 4.4, obtained from Appendix 2, the F value is computed as 35.82 and the p value is less than 0.0001. This means that there is a significant difference between these two pastes. Since there is significant difference between PV 145 and PV 159, which one is the better material for the screen printing step that should be recommended for use in the production process?

Table 4.4 The ANOVA table for pastes selection

Source	DF	Sum of Squares	Mean Square	F value	Pr> F
Model	1	0.00081684	0.00081684	35.82	<.0001
Error	253	0.00576913	0.0000228		
Corrected Total	254	0.00658597			

To determine which paste is better, the following statement was used in the SAS program.

ESTIMATE 'H0: PV145 = PV159' PV 1 -1;

Suppose that we could assume that the variances of the converting efficiency were identical

for both levels of the PV. Then, the appropriate test to use for comparing the two means is two-sample *t*-test. From the SAS results report, the P-value of t-test is smaller than 0.0001, which means that there is significant difference between the two PV types. Furthermore, looking at the estimated difference between the means (which is 0.00366584); one can say that PV145 is a better choice to improve the conversion efficiency. Therefore, the supplier's claim is inaccurate.

Table 4.5 The ANOVA table for pastes selection

Parameter	Estimate	Standard Error	t Value	Pr> | t |
H0: PV145 = PV159	0.00366584	0.00061249	5.99	<.0001

The confidence interval for the difference between the mean efficiency of PV 145 and PV 159 is shown as below:

4.2.4 Comparison of Pastes at Different Temperature Values

For the screen printing step, there is another factor of interest to the engineers, different levels of temperature setting. The lower the temperature used the more savings in electricity usage. Besides, the R&D engineers also would like to know if there is any significant interaction

effect between different pastes and different temperatures.

- **Data description**

For testing the combination of different pastes and different temperatures, we used the first finger printing method, 65 fingers with 80 um width and 153 lengths. In this experiment, there are three settings for the temperature, which results in six combinations of the two factors under study. Here too 1,186 observations were obtained randomly by an Excel function.

- **The model for different pastes with different temperatures**

,

.

is a constant common to all observations

are the effect of different pastes, = 1, 2

are the effect of different temperatures, = 1, 2, 3

are the effect of interaction between pastes and temperatures

represent the random error

represent the solar cell conversion efficiency for paste and observation

represent the effect of different pastes. represent the effect of different temperatures.

are the interaction effects between pastes and temperatures. Conversion efficiency

( ) represents the tested converting efficiency. are the random error terms that are assumed to be independently and identically distributed ~N (0,).

- **ANOVA Table**

From Table 4.6, obtained from Appendix 3, the F value is computed as 11.28 and the p-value is less than 0.0001. It can be concluded that there is significant difference between the pastes and temperatures. Therefore, it is necessary to further analyze the results to discover the difference between various factor levels that are significantly different from each other.

Table 4.6 The ANOVA table for two pastes and three temperatures

Source	DF	Sum of Squares	Mean Square	F value	Pr> F
Model	5	0.00357081	0.00071416	11.28	<.0001
Error	1180	0.07467593	0.00006328		
Corrected Total	1185	0.07824674			

From Table 4.7, obtained from Appendix 3, the F value of PV is computed as 49.52 and p-value is less than 0.0001. It can be concluded that PV paste factor significantly influence the converting efficiency. Therefore, the type of paste is an important factor that has to be considered. The F value of the Temperature is computed as 1.23 and the p value is 0.2920 which is larger than 0.05. It means that the Temperature in this model is insignificant. In other words, the Temperature would not influence the conversion efficiency significantly.

Table 4.7 The ANOVA table for PV, Temperatures and their Interaction

Source	DF	Type I SS	Mean Square	F value	Pr> F
PV	1	0.00313397	0.00313397	49.52	<.0001
Temperature	2	0.00015599	0.00007799	1.23	0.2920
Interaction PV* Temperature	2	0.00028085	0.00014042	2.22	0.1092

Also, from table 4.7, the F value of the PV and temperature interaction is computed as 2.22 and p value is 0.1092 which is larger than 0.05. It means that the interaction between PV and temperature is not statistically significant. In other words, different temperatures combined with different pastes would not influence conversion efficiency. In conclusion, the result of combination of paste types with different temperatures is that only the pastes should be considered, the temperature setting in screen printing step would not influence the conversion efficiency. Besides, the interaction of pastes and temperature can be ignored in this production step. Since it was found that only paste type is a significant factor, it is unnecessary to do further analysis of temperature.

4.3 Result and Discussion

From the view point of a company, it is preferred to continue the manufacturing process while experimentation is in progress without any interruption. However, in order to get the

needed experimental data, the engineers have to interrupt production at certain periods of time to run the experiments. Therefore, conducting the experiments would be considered a component of research cost for the company. Most companies would require the engineers to minimize interruption due to experiments so that the manufacturing output would be better and bring positive benefits. Therefore, most of the times, these kinds of experiments cannot be conducted frequently and they should be done on a limited scale. Besides, it is better that products made during experimentation can be sold. Hence, the number of data sets obtained is limited to a few hundred only. Even with limited data, engineers still have to be able to perform correct analysis and reach accurate conclusions. Based on the experimental results from testing finger printing methods, paste selection and different pastes with different temperatures, by using ANOVA table with SAS system, the engineers can assess various factor effects from these combinations. The ANOVA table clearly defined the relationship among these factors, and showed that the first screen printing method is the preferred method for the solar cell efficiency. By using the first screen printing method, the PV 145 would be selected as the paste to be used because its efficiency is significantly better than paste PV 159. Furthermore, the paste types with different temperatures were also analyzed by the ANOVA table and it was concluded that different paste types printed with different temperatures would not influence the conversion efficiency significantly.

5. Conclusions and Future Work

This research was aimed at the construction and application of statistical methods that can be used to compare various production methods and related manufacturing factors at Ever Energy Corporation's production line.

Statistical analysis of data collected at the company's production facility showed that among the 3 finger printing forms, Method 1, i.e. 65 fingers, 80μm in width and 153mm in length, is the most advantageous method. This conclusion is in agreement with the selection made by Ever Energy Corporation. The use of this method results in the generation of the highest conversion efficiency with optimal number of fingers and surface area.

R&D engineers in Ever Energy Corporation suggested choosing a new paste type PV159 over the old paste type, PV145, solely based on properties of the new paste such as conductivity and converting efficiency after sintering, as well as comparisons between some preliminary figures and their personal experience. However, by using statistical analysis methods, it was demonstrated that new paste type PV159 does not out-perform the old paste type PV145, which is also economically more advantageous. This recommendation, if adopted, could result in significant cost savings for the company.

The effect of paste types (two levels), temperature (three levels) and their interaction was also studied. Six combinations of paste and temperature settings (i.e. 2 pastes types and

3 temperature settings at 860^0C, 875^0C, and 890^0C) were studied. While the R&D engineers at Ever Energy Corporation consider PV159 and 890^0C as the most appropriate combination, statistical analysis in this report pointed out that temperature is not a statistically significant factor, indicating that a relatively lower temperature could potentially generate the same conversion efficiency. This could potentially result in significant cost savings for the company.

In conclusion, although the use of statistical methods and application of the design of experiments methodology is crucial, it must be noted that all findings of this project must be validated and improved upon in the future. It is important to work with the production line engineers to explore other variables and possibly extend the results of the current project to more factors and production settings.

6. References

[1] Dai, S.-P., Study of amorphous/crystalline silicon heterojunction solar cells. July 2007, National Dong Hwa University, Taiwan.

[2] Yang, J.-K., Efficiency measurement systems and performance parameters of photovoltaic devices. July 2005, National Dong Hwa University.

[3] Martins, A.C., R.C. Marques, and C.O. Cruz, Public-private partnerships for wind power generation: The Portuguese case. Energy Policy. **39**(1): p. 94-104.

[4] Devine-Wright, P., Enhancing local distinctiveness fosters public acceptance of tidal energy: A UK case study. Energy Policy. **39**(1): p. 83-93.

[5] Chun, C., The study of the solar cells. 2008: CHWA.

[6] Zhao, J.H., et al., 24% efficient PERL silicon solar cell: Recent improvements in high efficiency silicon cell research. Solar Energy Materials and Solar Cells, 1996. **41-2**: p. 87-99.

[7] Lipinski, M. and P. Panek, Optimisation of monocrystalline silicon solar cell. Opto-Electronics Review, 2003. **11**(4): p. 291-295.

[8] Zhao, J.H., et al., A 19.8% efficient honeycomb multicrystalline silicon solar cell with improved light trapping. Ieee Transactions on Electron Devices, 1999. **46**(10): p. 1978-1983.

[9] Zhao, J.H., et al., 19.8% efficient "honeycomb" textured multicrystalline and 24.4% monocrystalline silicon solar cells. Applied Physics Letters, 1998. **73**(14): p. 1991-1993.

[10] Szlufcik, J., et al., Low cost industrial technologies of crystalline silicon solar cells. Proceedings of the Ieee, 1997. **85**(5): p. 711-730.

[11] Elnahwy, S., N. Adeeb, and N. Rafat, AN OPTIMUM BASE DRIFT FIELD FOR A P-N-JUNCTION SOLAR-CELL. Journal of Physics D-Applied Physics, 1990. **23**(1): p. 112-117.

[12] Chiao, S.C., J.L. Zhou, and H.A. Macleod, OPTIMIZED DESIGN OF AN ANTIREFLECTION COATING FOR TEXTURED SILICON SOLAR-CELLS. Applied Optics, 1993. **32**(28): p. 5557-5560.

[13] C.Y.Tsai, High Efficiency Solar Cell.

[14] Chen, S., The study of rapid in-line PECVD SiNx:H antireective coating layer on the commercial crystalline silicon solar cells. June 2004, National Cheng Kung University, Taiwan.

[15] Jeon, S.J., S.M. Koo, and S.A. Hwang, Optimization of lead- and cadmium-free front contact silver paste formulation to achieve high fill factors for industrial screen-printed Si solar cells. Solar Energy Materials and Solar Cells, 2009. **93**(6-7): p.

1103-1109.
[16] Kyeong, D., et al., Laser Edge Isolation for High-efficiency Crystalline Silicon Solar Cells. Journal of the Korean Physical Society, 2009. **55**(1): p. 124-128.
[17] Schon, J., et al., Analysis of simultaneous boron and phosphorus diffusion gettering in silicon. Physica Status Solidi a-Applications and Materials Science. **207**(11): p. 2589-2592.
[18] Grauvogl, M., A.G. Aberle, and R. Hezel, 17.1% efficient metal-insulator-semiconductor inversion layer silicon solar cells using truncated pyramids. Applied Physics Letters, 1996. **69**(10): p. 1462-1464.
[19] Erath, D., et al., Advanced screen printing technique for high definition front side metallization of crystalline silicon solar cells. Solar Energy Materials and Solar Cells. **94**(1): p. 57-61.
[20] Kwon, T., et al., The effect of firing temperature profiles for the high efficiency of crystalline Si solar cells. Solar Energy Materials and Solar Cells. **94**(5): p. 823-829.
[21] Cooper, I.B., et al., Understanding of High-Throughput Rapid Thermal Firing of Screen-Printed Contacts to Large-Area Cast Multicrystalline Si Solar Cells. Ieee Transactions on Electron Devices. **57**(11): p. 2872-2879.
[22] Rohatgi, A. and J.W. Jeong, High-efficiency screen-printed silicon ribbon solar cells by effective defect passivation and rapid thermal processing. Applied Physics Letters, 2003. **82**(2): p. 224-226.
[23] Doshi, P. and A. Rohatgi, 18% efficient silicon photovoltaic devices by rapid thermal diffusion and oxidation. Ieee Transactions on Electron Devices, 1998. **45**(8): p. 1710-1716.
[24] Kray, D., Modeling, geometric optimization and isolation of the edge region in silicon solar cells. Solar Energy Materials and Solar Cells. **94**(5): p. 830-835.

7. Appendix

Appendix 1

The GLM Procedure

Class Level Information

Class	Levels	Values
Method	3	1 2 3

Number of Observations Read	279
Number of Observations Used	279

The SAS System

The GLM Procedure

Source	DF	Sum of Squares	Mean Square	F Value	Pr > F
Model	2	0.00117304	0.00058652	45.95	<.0001
Error	276	0.00352297	0.00001276		
Corrected Total	278	0.00469601			

R-Square	Coeff Var	Root MSE	y Mean
0.249795	2.195082	0.003573	0.162761

Source	DF	Type I SS	Mean Square	F Value	Pr > F
Method	2	0.00117304	0.00058652	45.95	<.0001

Source	DF	Type III SS	Mean Square	F Value	Pr > F
Method	2	0.00117304	0.00058652	45.95	<.0001

Parameter	Estimate	Standard Error	t Value	Pr > |t|
H0: M1 = M2	0.00508486	0.00053046	9.59	<.0001
H0: M2 = M3	-0.00263352	0.00052916	-4.98	<.0001
H0: M1 = M3	0.00245134	0.00051435	4.77	<.0001

Appendix 2

The GLM Procedure

Class Level Information

Class	Levels	Values
PV	2	1 2

Number of Observations Read	255
Number of Observations Used	255

The SAS System

The GLM Procedure

Source	DF	Sum of Squares	Mean Square	F Value	Pr > F
Model	1	0.00081684	0.00081684	35.82	<.0001
Error	253	0.00576913	0.00002280		
Corrected Total	254	0.00658597			

R-Square	Coeff Var	Root MSE	y Mean
0.124028	3.018046	0.004775	0.158223

Source	DF	Type I SS	Mean Square	F Value	Pr > F
PV	1	0.00081684	0.00081684	35.82	<.0001

Source	DF	Type III SS	Mean Square	F Value	Pr > F
PV	1	0.00081684	0.00081684	35.82	<.0001

Parameter	Estimate	Standard Error	t Value	Pr > |t|
H0: PV145 = PV159	0.00366584	0.00061249	5.99	<.0001

Appendix 3

The GLM Procedure

Class Level Information

Class	Levels	Values
PV	2	1 2
Temperature	3	1 2 3
pvtemp	6	1 2 3 4 5 6
Number of Observations Read		1186
Number of Observations Used		1186

The SAS System

The GLM Procedure

Source	DF	Sum of Squares	Mean Square	F Value	Pr > F
Model	5	0.00357081	0.00071416	11.28	<.0001
Error	1180	0.07467593	0.00006328		
Corrected Total	1185	0.07824674			

R-Square	Coeff Var	Root MSE	y Mean
0.045635	5.063421	0.007955	0.157111

Source	DF	Type I SS	Mean Square	F Value	Pr > F
PV	1	0.00313397	0.00313397	49.52	<.0001
Temperature	2	0.00015599	0.00007799	1.23	0.2920
pvtemp	2	0.00028085	0.00014042	2.22	0.1092